JCMM
Available online at
www.jcmm.ro
www.jcmm.org

J. Cell. Mol. Med. Vol 10, No 1, 2006 pp. 145-156

Neuroglia in the inferior olivary nucleus during normal aging and Alzheimer's disease

H. Lasn, B. Winblad, N. Bogdanovic *

Section for Clinical Geriatric, NEUROTEC Institutionen, Karolinska Institutet, Stockholm, Sweden

Received: November 24, 2005; Accepted: February 14, 2006

Abstract

It is likely that neuronal loss occurs in certain brain regions in Alzheimer's Disease (AD) without any neurofibrillary pathology. In the human principle inferior olivary nucleus (PO), we have shown that neuronal loss is about 34% (Lasn et al. Journal of Alzheimer Disease, 2001; 3: 159-168), but the fate of the neuroglial cells is unknown. Since the unique network of neurons and neuroglial cells and their cohabitation are essential for normal functioning of CNS, we designed a study to estimate the total number of oligodendrocytes and astrocytes in normally aged and AD brains. The study is based on 10 control and 11 AD post-mortem human brains. An unbiased stereological fractionator method was used. We found significant oligodendroglial cell loss (46%) in AD as compared to control brains, while the total number of astrocytes showed a tendency to decrease. It is likely that the ratio of oligodendroglial cells to neurons remains unchanged even in degenerative states, indicating that oligodendroglial cells parallel neuronal loss. Astroglial cells did not increase in total number, but the ratio to neurons was significantly increased due to the neuronal loss. Using a novel unbiased quantitative method, we were able to describe significant oligodendroglial loss in the PO but the pathogenic mechanism behind remains unknown.

Keywords: astrocyte • oligodendrocytes • quantification • stereology • dementia • neurodegeneration

Introduction

Alzheimer disease (AD) is the most common form of adult onset dementia and is characterized by the accumulation of extracellular neuritic plaques (NPs) and intraneuronal neurofibrillary tangles (NFTs), both considered as pathological hallmarks of AD in the disease-specific brain regions [1–3]. In addition, neuronal loss [2, 4], synaptic loss [5], reactive astrocytosis [3, 5–7], activated microglia [3] and oligodendroglial degeneration [8] are usually found in AD brains. Although AD is considered to be a neurodegenerative disorder, its pathogenesis and etiology remain elusive. Until today most morphological studies have focused on brain areas affected by NPs and NFTs, while very few reports are available about the other so-called "non-classically" affected areas.

Pathological changes of NFTs and NPs follow a unique staging pattern described in detail by Braak [9]. Much less NP and NFT pathology has been found in brainstem regions as compared to classically affected brain regions [10] and the NFT presence in raphe nuclei correlates to cortical stages in AD [11]. The vulnerability of neuronal cells is not considered to depend on neurotransmitter type but rather to be due to the fact that neurons with long

* Correspondence to: Assoc. Prof. Nenad BOGDANOVIC
Karolinska Institutet, Neurotec,Geriatric Department,
NOVUM, plan 5, 14186 Stockholm Sweden.
E-mail: Nenad.Bogdanovic@ki.se

and sparsely myelinated axons are more susceptible to AD pathology than neurons with shorter and well-myelinated axons [12]. Some brainstem regions, such as the inferior olivary complex show no neurofibrillary pathology. Despite this fact the inferior olivary complex shows a significant neuronal loss up to 34% [13].

The cause of neuronal loss in the PO is not known. Neuronal function depends upon the balance and interaction of other supportive cells, such as astrocytes and oligodendrocytes, in the vicinity of the neurons [3, 14–19]. As far as we know, there are no reports focusing on the destiny of neuroglial cells in the PO in AD or aging. Using stereological method, Pakkenberg *et al.* could not estimate any changes in total number of neuroglial cells in the aging human cortex or in AD [20, 21].

The aim of this study was to use a novel design-based stereological method called the optical fractionator to estimate the total number of astrocytes and oligodendrocytes in the PO in AD and in normally aging brains.

Material and methods

The study was based on 10 normal control and 11 AD post-mortem human brains obtained from the Huddinge Brain Bank, Stockholm, in accordance with Swedish law and the permission of the Karolinska University Hospital Ethical Committee. The control group included the brains of subjects who did not die of neurological or psychiatric diseases and who had no history of long-term illness (mean age was 54 years, range 17–79 years). Furthermore, the control group was divided into two subgroups: young controls (CY) 17–57 years, mean age 41 years and older controls (CO) 69-79 years, mean age 73 years. Of note, the CO group did not have any neuropathological features of AD, such as neurofibrillary changes in trans-/entorhinal region or amyloid plaques in the cortex. The AD group included brains from patients with clinically and pathologically confirmed AD (mean age 85 years, range 67–92 years). Additionally, the AD group was divided into age-matched and older AD. Clinical diagnosis was based on combined DSM-III-R [22] and NINCDS-ADRDA criteria [23]. The definite neuropathological diagnosis of AD was determined by using CERAD and NIA-Reagan Institute Criteria [24–26]. Brains from AD patients with clinical signs of Parkinson-like symptomatology and the brains with other major neuropathological co-findings, *e.g.* multi-infarction or presence of Lewy bodies, were excluded from the analysis. All the brains were fixed within 24–48h of death. We are aware that total AD group is older than CO group but clinical duration of Alzheimer´s disease did not differ between two AD subgroups: matched AD and old AD (7,6 years in both subgroups). Thus these groups were analysed as only one AD group. The complete demographic data are shown in Table 1.

The absence of NFTs or NPs in the PO was excluded by routine diagnostic procedure at the Huddinge Brain Bank [24]. All the brains were used in our previous stereological study, which estimated the total number of neurons in the PO [13]. In addition, we analyzed 2 cases with known AD related gene mutation each (Swedish $_{670/671}$ and PS-1) by routine neuropathological methods.

Sectioning and histology

After fixation in 4% buffered formaldehyde (pH 7,4), the inferior olivary complex was embedded in paraffin, thereafter cut exhaustively in a randomly chosen saggital plane on the microtome into a series of 30 μm thick sections. The sections were stained with Nissl staining solution [0,5% cresyl-violet in distilled water (ratio 1:4)] The mounted sections were placed in the staining solution until adequate intensity of staining was achieved. After that, they were rinsed in distilled water twice for 5 minutes, thereafter through a graded series of alcohol solutions: 50% ethanol, 70% ethanol with a few (2–4) drops of 25% acetic acid, 70% ethanol, and 95% ethanol, for 10 minutes each. Finally, the sections were placed in 2 parts ether to 1 part absolute alcohol for 5 minutes, rinsed in xylene for 5 minutes, and mounted with a cover glass using Permount mounting medium. The presence of amyloid plaques and amyloid angiopathy was detected with polyclonal antibody for Aβx-42 and Aβx-40 (each 1:1000, kindly provided by J. Näslund, [27]). For detecting abnormal tau formation we used monoclonal antibody for AT8 (1:200, Innugenetics, Belgium) and Gallyas silver iodide stain [33]. After incubation of the different primary antibodies, the sections were treated with a biotinylated secondary antibody (1:300, DAKO). and visualized with the avidin-biotin-peroxidase complex kit (Vector, Burlinggame, Calif.) with 3,3'-diaminobenzidine-4HCl/H2O2 (DAB, Sigma, St.Louis, Mo.) as a substrate. Thereafter the sections were counterstained with hematoxylin-eosin stain for background. Negative control slides for all antibodies were treated in an identical manner, except for incubation without a primary

antibody. As a positive control staining, the sections of cerebral cortex affected by AD pathology were used.

Morphological criteria for astroglia and oligodendroglia.

The neuroglial cells could be easily differentiated from neurons in the PO since the latter have a nucleus with a single large nucleolus, no heterochromatin, and a round nucleus with visible cytoplasm [28, 29]. Oligodendrocytes are determined by smaller round or oval dark nuclei with dense chromatin, and they are usually in close proximity to neurons. The astrocytes were defined as cells with bigger, paler and less densely packed heterochromatin, without a clear nucleolus and showing a patchy pattern of granules in a rim below the nuclear membrane. On Nissl staining, the size and shape of the neuroglial cells make them clearly distinguishable from the neuronal population. Microglia showed small elongated or comma-shaped nuclei with dense peripheral chromatin, which makes them easy to distinguish from other neuroglial cells and from neuronal cells (for more details see [29]).

Quantification

To estimate the total number of astrocytes and oligodendrocytes in the PO, we applied a stereological approach - random systematic sampling and the unbiased optical fractionator method [30], using a similar experimental design as that reported previously [13]. By using an optical dissector probe, it is possible to sample isolated particles, in this case astrocytes and oligodendrocytes, with a uniform probability in the three-dimensional space, regardless of the size, shape or orientation of the tissue. Briefly, the area of interest was delineated in low magnification (x2.5) using the cursor. Due to the clear anatomical borders, it is not difficult to distinguish the human PO from its surrounding regions. A meander sampling function of the GRID v2.0 program (Olympus, Denmark) was used for stepping through the delineated area with a chosen counting frame. Then, a 100-x oil-immersion objective with a numerical aperture of 1.40 was moved into place and the appropriate counting frame superimposed on the screen. The desired horizontal and vertical step lengths, assisted by a highly precise servo-controlled motorized microscopy stage, were dimensioned for the appropriate distance [=600 μm (x step) x 600 μm (y step)] in between the counting frames (280 μm^2). The cells in the space were counted by an optical dissector probe (z-axis) with a height of 15 micrometers of the total thickness of the section (26–29 μm). The thickness of every section was measured at three randomly chosen places to get the mean value of section thickness. According to the rules of stereology we counted between 150–200 cells per whole structure [31]**.** This procedure ensured the selection of a systematic random sample of sections, in which all parts of the PO had equal probabilities of being presented [30, 32]. Finally, the total number of oligodendrocytes and astrocytes per region was estimated according to the following equation:

$$N_{total} = \sum Q - \text{ x } 1/tsf \text{ x } 1/asf \text{ x } 1/ssf$$

$\sum Q-$ = the number of cells in a known fraction of the volume of the structure, *i.e.*, the known fraction of the total number of glial cells

tsf = thickness sampling fraction , h/T (height of dissector/section thickness)

asf = area (frame)/area (Δx x Δy step) is an area sampling fraction, *i.e.*, the area of the counting frame relative to the area associated with each step of the stepping motors.

ssf = section sampling fraction, (1/20) section sampled by a known fraction, yielding finally 5 sections per brain to be analysed.

Statistics

Statistical analyses of the results were performed using StatView 5.0.1 software. To analyze the differences between CY, CO, matched AD and old AD we used non-parametric Kruskal-Wallis test. To compare the number of oligodendroglial and astrocytic cells separately between the groups: CY *vs* CO; CY *vs.* total AD; CO *vs.* total AD the unpaired Mann-Whitney test was applied. For all tests the 0,05 level of significance was chosen. The two AD groups are taken together since there was no significant difference in age-matched and old AD in total glial number and duration of the disease. Precision of estimates was evaluated by calculating the coefficient of error (CE=SEM/mean) A satisfactory level is around 10% or less. The Spearman correlation coefficient (r) was used to estimate the relation between the following: a) age *vs.* oligodendrocytes, b) age *vs.* astrocytes, c) neuron *vs.* oligodendrocytes, d) neuron *vs.* astrocytes. The relation and accuracy are presented as the r, and p values. A $p<0,05$ was chosen as the criterion for the level of significance.

Table 1 The complete demographic data

Normal aging	Case no.	CERAD	Cause of death	Age (years)	disease duration (y)	Braak stage	Sex	Astrocytes x 10^6
control younger (CY)	1	control	Aneusysma aorta	17			M	12,4
	2	control	CO poisoning	38			M	12,8
	3	control	suicid	39			M	7,2
	4	control	Traffic accident	42			M	9,1
	5	control	insuff cardio-pulm	55			M	10,5
	6	control	alcoholism	57			M	10,7
mean N				41				10,5
SD				13				2,1
SEM								0,8
CE (%)								8
control older (CO)	7	control	Heart infarct	71			F	8,8
	8	control	traffic accident	79			M	9,8
	9	control	accident	69			M	9,1
	10	control	traffic accident	73			M	9,2
mean N				73				9,2
SD				4,3				0,4
SEM								0,21
CE (%)								2
total goup mean				54				10,0
SD				19				1,7
SEM								0,5
CE (%)								5
AD								
matched AD	11	def.AD	insuff cardio-pulm	67	7	5\6	M	8,8
	12	posAD	bronchopneumonia	79	6	5	M	5,7
	13	defAD	insuff cardio-pulm	82	9	6	F	5,9
	14	def.AD	bronchopneumonia	83	8	6	F	125,8
	15	def.AD	insuff cardio-pulm	83	8	6	F	
mean N				78				7,6
SD				6,7				2,7
SEM								1,23
CE (%)								16
old AD	16	def.AD	insuff cardio-pulm	86	8	4/5	F	5,9
	17	def.AD	urinary infection	90	7	6	F	13,24,4
	18	def.AD	bronchopneumonia	90	9	4/5	F	13
	19	proAD	card insuff	90	8	4	M	6,8
	20	pro/defAD	bronchopneumonia	90	7	4/5	M	10
	21	proAD	card insuff	92	7	4/5	F	
mean N				89	7,6			8,8
SD				1,9	0,8			3,7
SEM								1,53
CE (%)								17
Total AD mean N				84,7				8,3
SD				7,2				3,2
SEM								0,98
CE (%)								12

Def AD, pro AD, (definite, probable AD, respectively) indicate the diagnostic level of Alzheimer's disease according to Mirra *et al.* 1993. N = total number of neurons, SD = standard deviation, mean CE = mean coefficient of error of all individual estimates (CE = SEM/mean). Ratio O/N = ratio oligodendrocytes/neuron, ratio A/N = ratio astrocytes/neuron. The

Ologo x 10^6	Neuron x 10^6 *	ratio O/N	ratio A/N
5,1	0,77	6,6	16,1
9,2	0,97	9,5	13,2
3,2	0,64	5,0	11,3
5,5	0,69	8,0	13,2
3,8	0,83	4,6	12,7
4,5	0,69	6,5	15,5
5,2	0,76	6,7	13,6
2,3	0,12	1,8	1,8
0,9	0,049	0,8	0,7
17	6	11	5
4,8	0,61	7,9	14,4
4,1	0,41	10,0	23,9
4,5	0,82	5,5	11,1
3,5	0,69	5,1	13,3
4,2	0,6	7,1	15,7
0,56	0,17	2,3	5,6
0,28	0,086	1,1	2,8
7	14	15	18
4,9	0,7	6,8	14,5
1,8	0,2	1,9	3,6
0,6	0,05	0,6	1,2
12	7	9	8
5	0,53	9,4	16,6
2,6	0,61	4,3	9,3
1,8	0,41	4,4	14,4
2,2	0,39	5,6	30,8
1,5	0,47	3,2	12,3
2,6	0,48	5,4	16,7
1,4	0,09	2,4	8,3
0,62	0,04	1,1	3,7
24	8	20	22
2,7	0,32	8,4	18,4
3	0,4	7,5	33,0
2	0,4	5,0	11,0
2,9	0,41	7,1	31,7
3,3	0,27	12,2	25,2
1,6	0,3	5,3	33,3
2,6	0,35	7,6	25,4
0,7	0,06	2,6	9,1
0,27	0,03	1,1	3,7
10	8	14	15
2,7	0,4	6,6	21,5
1	0,99	2,6	9,5
0,30	0,03	1,10	2,90
11	7	17	13

neuronal number is from our previous study (Lasn *et al.*, 2001) where the same brains were used. Braak staging range from I-VI

Results

Oligodendroglia

Oligodendrocytes are characterized by a dark round-shaped nucleus and a barely visible cytoplasm. The distinction between neurons and glial cells can be seen on low magnification (Fig 1a, b). In control brains the oligodendroglial cells are scattered in the neuropil and they satellite around neuronal soma (Fig.1c). The most striking difference between the control and AD brains was the location of oligodendrocytes with respect to neurons. This phenomenon is not generally seen in AD (Fig 1d). We calculated the ratio of oligodendrocytes to neurons, and the result did not differ between control and AD group (see Table 2).

There was no difference in the total number (mean ± SD) of oligodendrocytes between the younger ($5,4x10^6 \pm 2,3$) as compared to the older ($4,2x10^6 \pm 0,6$) controls. The mean total number of oligodendrocytes in AD is $2,7x10^6 \pm 1,0$ which shows significant decline of oligodendroglial cells by 46% in AD.(Fig. 2).

When all cases (AD and controls) are plotted, the total number of oligodendroglial cells is positively correlated to the number of neurons ($r=0,68$; $p=0,02$). (Fig. 3).

Astrocytes

Nissl staining showed no difference in the morphological features of the astroglial cells (Fig. 1c, d). Histologically, a visual observation might suggest a larger number of astrocytes in AD cases, but the stereological estimation indicated no significant difference in the total number of astrocytes in control (both groups included) *vs.* AD group, $10 x10^6 \pm 1,7$ *vs.* $8,0x10^6 \pm 3,2$ (mean ± SD), respectively. The mean estimate of the number of astrocytes in AD is lower than in controls, but this decrease does not reach significance (Fig. 2). There is no correlation between total number of astrocytes and total number of neurons ($r=0,25$; $p=0,27$) (Fig. 3). Furthermore we estimated the ratio between astrocytes and neurons in all investigated groups. While the ratio was not changed for the control groups, the AD group displayed a significant increase of 48% (from 14,5 to 21,5 Table 2).

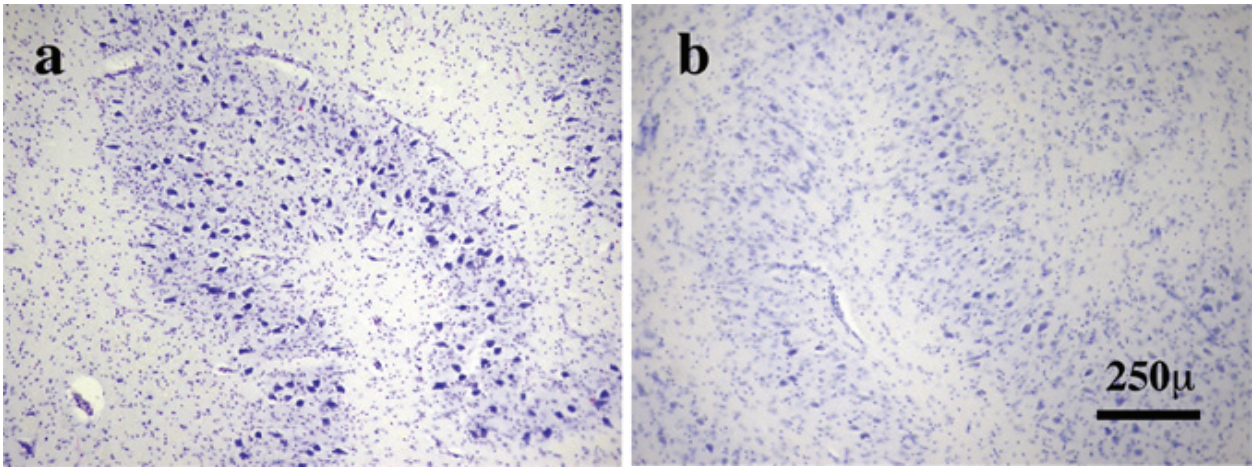

Fig. 1 Photomicrograph represents low (**a, b**) and high magnification (**c, d**) of olivary inferior nucleus in the control (**a, c**) and AD (**b, d**) human brain. Using Nissl staining, neurons (*), oligodendroglial cells (arrow) and astrocytes (double arrow) can be differentiated. At low magnification a clear difference in staining by Nissl is visible due to the neuronal loss and paler neurons in AD (**b**). At higher magnification note the presence of oligodendroglial cells in the vicinity of the neurons in the control brain (**c**). This phenomenon is absent in AD brain. Astrocytes can be distinguished since a characteristic pale nucleolus and chromatin pushed towards nuclear edges can be noted. Bar **a, b** = 250 µm, Bar **c, d** =20 µm.

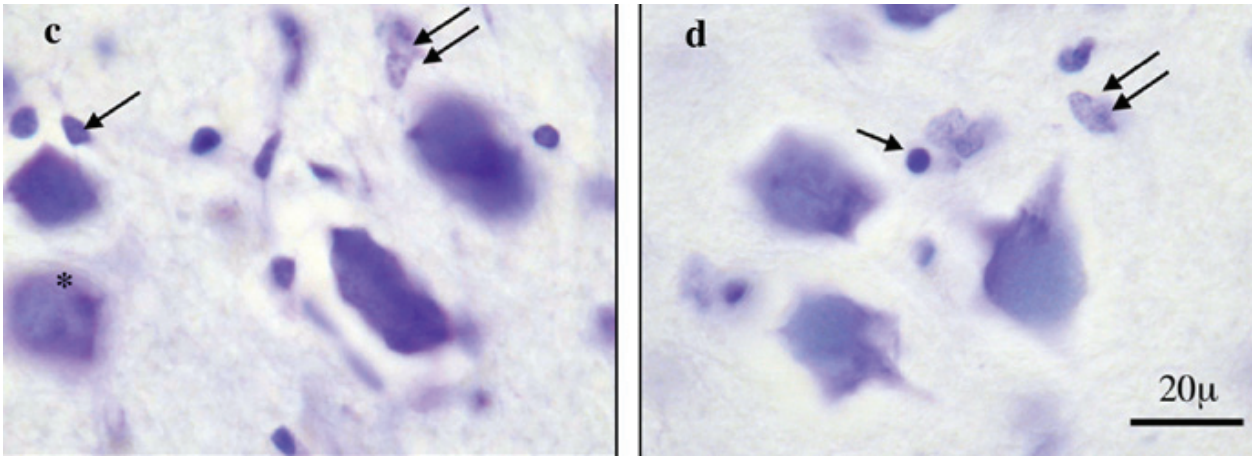

Table 2 Ratio of oligodendrocytes/neuron and astrocytes/neuron

	Neurons in AD	Neurons in CY	Neurons in CO
Oligodendrocytes	6,6	6,7	7,1
Astrocytes	21,5*	13,6	15,7

CY= young controls, CO = old controls
* The ratio between astrocytes and neurons in AD was increased for 48%. Control values were analysed as a mean of two groups (CY; CO). Control oligodendrocytes = 6,8 ± 1,9 and control astrocytes 14,5 ± 3,6

Neuroglial cells during aging

The total number of oligodendrocytes (r= -0,42; p=0,21) and astrocytes (r= -0,34; p=0,31) in the PO remained unchanged during normal aging in 10 control cases.

Gallyas staining

Using silver impregnation method by Gallyas [33] we unexpectedly found the globose-like tangle formation (Fig. 5) and scattered neurofibrillary treads in the neuropil in only one AD case (case No 17). That particular case was heavily affected by AD

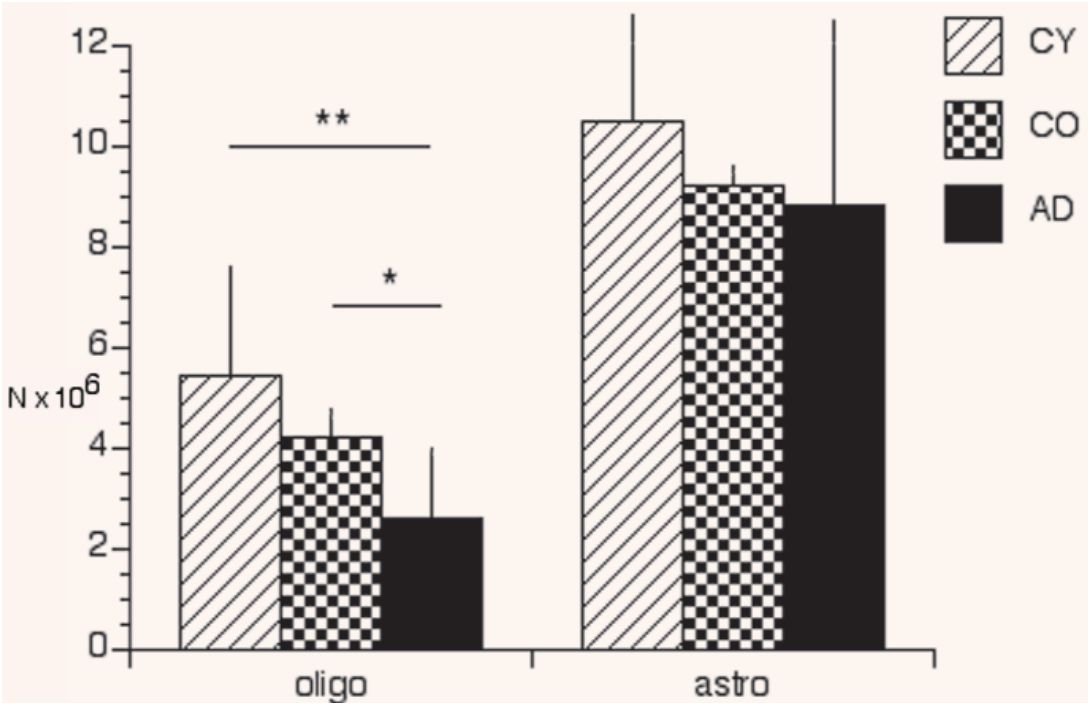

Fig. 2 The total number of oligodendroglial and astroglial cells in young (CY), old (CO) controls and in AD (mean ±SD). ** p<0.01, * p<0.05

(Braak stage VI) with clinical symptomatology of Alzheimer's disease without any other neurological symptoms. To test the hypothesis that globose tangles may appear in very affected AD cases the same staining was performed even on one Swedish mutation (Swedish $_{670/671}$) and one case of presenilin 1 (PS-1) mutation. None of our AD cases as well as mutation cases displayed any globose tangles but only argyrophilic granules scattered over the area of lipofuscin (Fig. 6b). This phenomenon was not found in any control case (Fig. 6a) but was strongly present in PS-1 case (Fig. 6c).

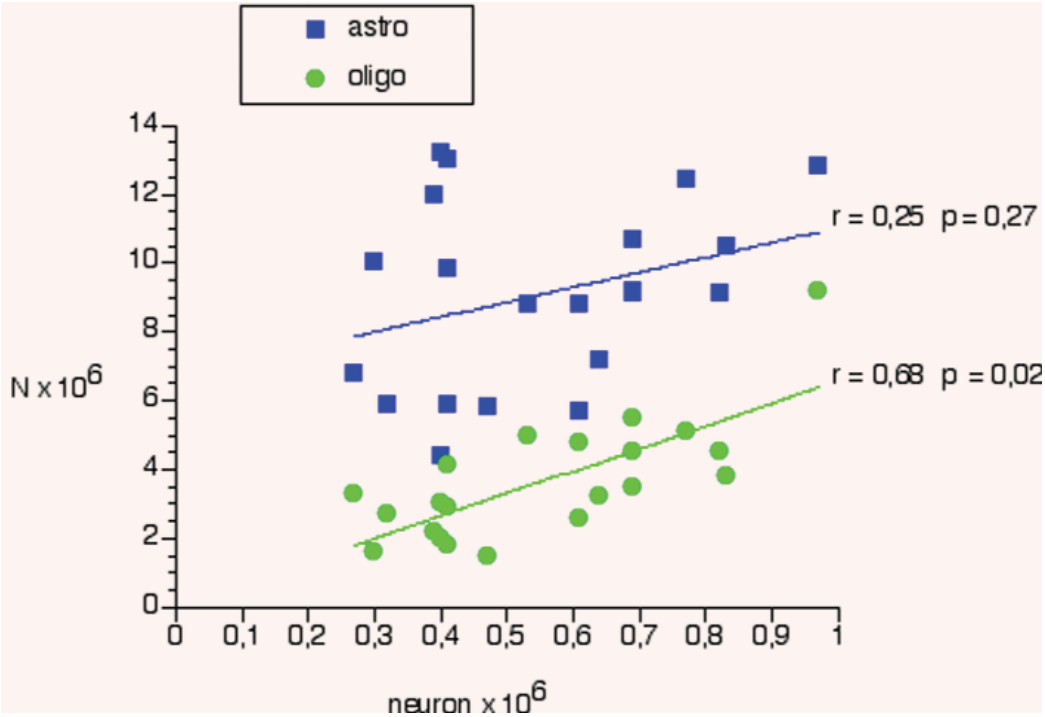

Fig. 3 The significant correlation was found only between oligodendroglial and neuronal cells. All control and AD cases are presented together.

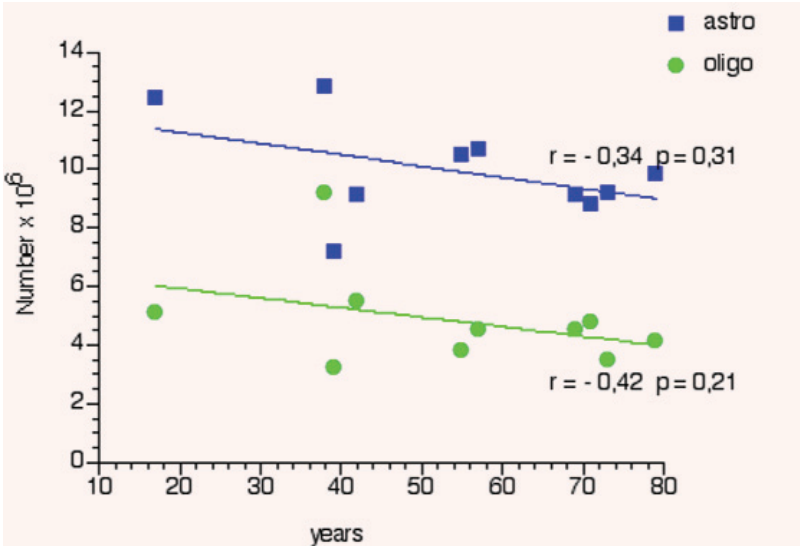

Fig. 4 There is no correlation neither in total number of oligodendrocytes nor astrocytes during aging in control group.

Tau staining with AT-8

The AT-8 staining was negative in control and all AD cases with exception of case nr. 17, where tangle staining was seen in some neurons and neuropil treads (not shown). In addition, no AT-8 positivity was obtained in any olivary neuron neither in Swedish $_{670/671}$ nor PS-1 mutation brains.

Amyloid staining

By immunostaining with $A\beta_{40}$ and $A\beta_{42}$ antibodies we could detect the presence of diffuse-like plaques in all AD cases, positive only for $A\beta_{42}$. No sign of amyloid angiopathy was noticed. The amyloid accumulation in grey matter was of different in size and intensity. The amount of plaque-like structures varied from 1 to maximally 5 per section. The plaques were scattered only in grey matter (Fig. 7) while in both mutation cases a more abundant presence of diffuse plaques was found in the grey and hilar white matter as well as in vessels (not shown).

Discussion

This study is presumably the first one to estimate the total number of neuroglial cells in the human

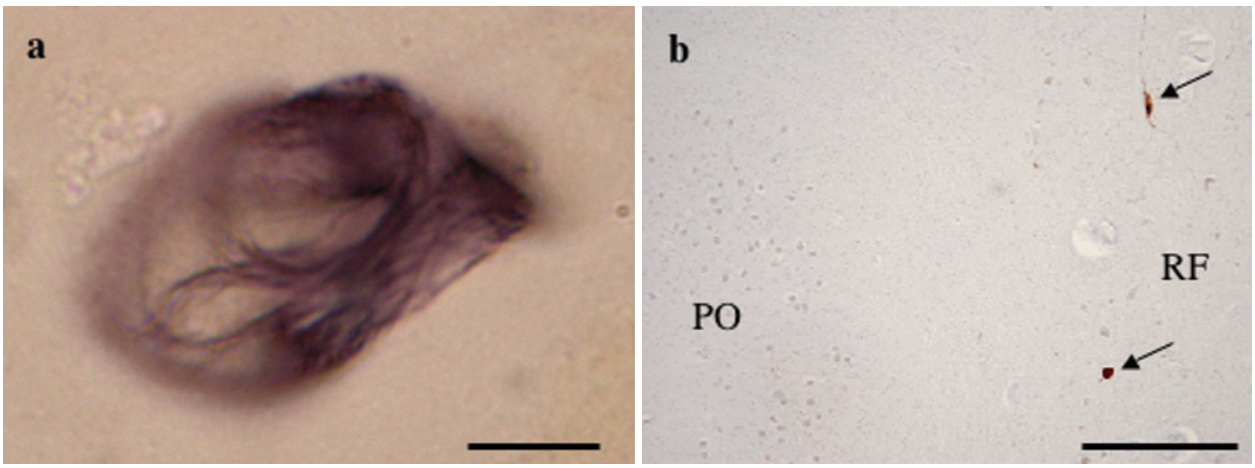

Fig. 5 Gallyas silver impregnation (**a**) shows a globose tangle in the olivary neuron in the AD case No17. A representative case of AD (**b**): AT-8 immunopositivity could not be found in the olivary region PO but in the neurons of reticular formation nearby. Bar **a** = 10 μm, Bar **b** =250 μm.

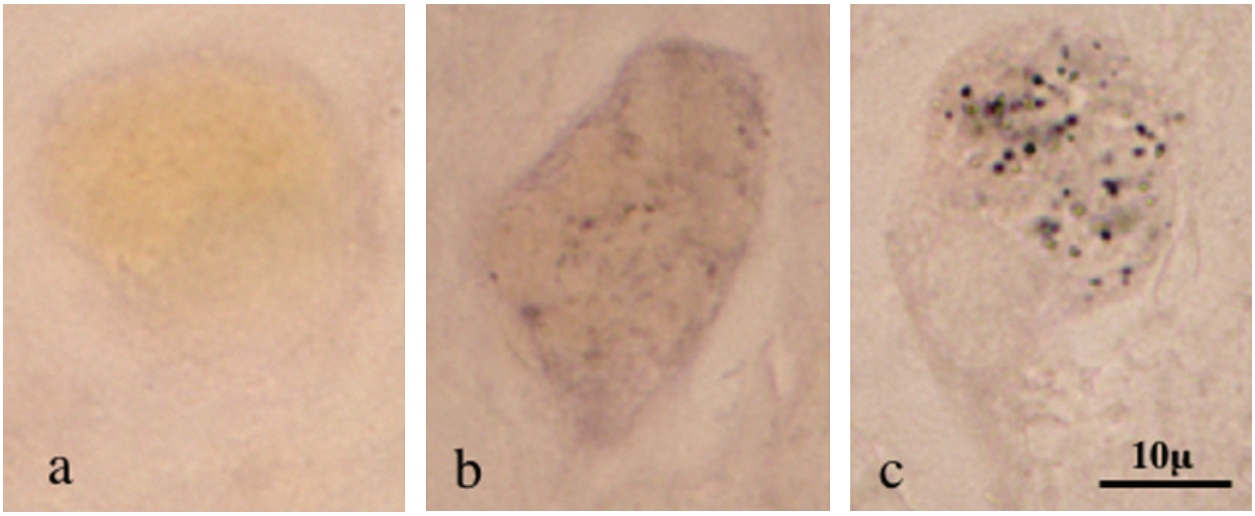

Fig. 6 Control case (**a**), representative AD (**b**) and AD with presenilin 1 mutation case (**c**). AT-8 positive granules were not found in control but in AD cases. Note that the argyrophilic granules are localized in the lipofuscin compartment especially plentiful in PS1. Bar **a**, **b**, **c** = 10 µm.

PO by using the modern unbiased stereology technique [30]. We found 46% decrease of oligodendroglial cells in AD. No decline was observed in the astroglial cell population, which remained stable in AD. Moreover, the oligodendroglial loss parallels a neuronal loss up to 34% in the PO (as previously reported in [13]). Since the neuron-glial interactions play an important role in information processing in the CNS, it is likely that an imbalance in one of these cell groups perturbs this morphofunctional neuron-glial network [34]. As previously reported, the proximity of the oligodendroglial cells to neurons plays an important role in the exchange of trophic factors and different forms of communication between these cell groups [35–37]. It is particularly interesting that oligodendrocyte - neuronal interaction is considered as a stabilizer for the neurons [14, 16, 38]. It is likely that a close oligoden-

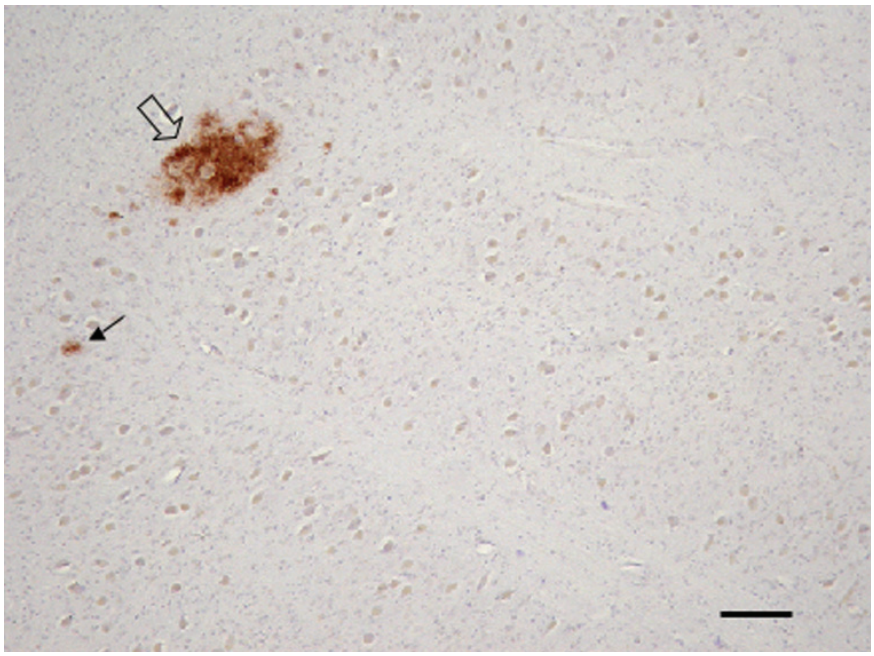

Fig. 7 Aβ-42 immunopositivity in the olivary nucleus in a representative AD case. The most of amyloid accumulations were small in size and few in number (arrow). Occasionally big diffuse-like plaques could be seen (open arrow). The open arrow is directed towards the biggest plaque found in our AD group. Bar = 100 µm

drocyte - neuronal cohabitation and the sharing of a common destiny is unique feature across the regions of the control and AD brains [20, 21].

Since the cohabitation of oligodendroglia and neurons is important for their existence, Heiko Braak has suggested that the loss of oligodendroglial cells could be a primary cause of AD [12] and presumably loss of oligodendroglial trophic support might lead to increased neuronal vulnerability. Whether the functional competence of oligodendrocytes could prohibit the development of AD remains obscure. Despite the presence of amyloid accumulation in our AD cases neither neurons nor oligodendrocytes stained positively with apoptotic marker Cytodeath 30 (data not shown) in PO. It is interesting that apoptotic events are not considered to be a main pathological event in different regions of AD brains [2] and dissimilarities between *in vitro* and *in vivo* studies are found [39].

The ratio of oligodendroglial cells to neurons in the PO is about 7:1 and remains stable among young and old controls, as well as in AD. In the cerebral cortex this ratio is about 1:1 [21]. Thus, more oligodendroglial cells around the olivary neurons might represent "better" protection against susceptibility to different hazardous events in CNS, which may be a feature of phylogenetically and ontogenetically older regions, such as the PO as compared to younger regions, such as the neocortex. Even in AD, the ratio between oligodendrocytes and neurons in the cerebral cortex remains unchanged (0.98) [21]. This may suggest that a lower neuron-glia ratio in the cortex correlates with a greater plasticity and "vulnerability" as suggested by Braak [12, 40], but also might suggest that the fates of neurons and oligodendroglia are interdependent. Some recent data have shown that oligodendrocytes are more vulnerable to Aβ toxicity and oxidative stress in AD [39]

In the present study we show that the absence of neurofibrillary tangles and threads but presence of amyloid plaques are common features in the PO in all AD cases with or without mutation history. Similar data has been reported previously [10, 41]. The presence of globose tangles in one single case of AD is a very unusual finding and needs to be further analyzed. Using conventional Gallyas staining method [39] we could vizualise the positive accumulation of argyrophilic granules, particularly in the PS1 mutation brain. The nature of these granules is still unknown but using the Gallyas-Braak modified method [42] the relation to lysosome-like structure is suggested [43]. Furthermore, the presence of a low amount of amyloid accumulation in PO is a common finding, with an exacerbation in the mutation cases [41]. These findings concerning tau and amyloid pathology in PO are intriguing since the lysosomal system has been suggested to be involved in pathogenic mechanism of both tau and amyloid pathways [44–48]. It could happen that diverse morphological phenotypes, with regional and cellular differences, are exposed to the same underlying pathogenic mechanism.

The number of astrocytes in the PO does not change during aging, but seems to display a non-significant tendency to decrease in AD. We have noted large inter-individual differences among the AD cases but we could not relate them to specific tau or amyloid pathology. There are no reported studies of the PO using the same quantitative experimental design for neurodegenerative disorders. There are few qualitative observations where a similar astrocytic "passivity" has been noted in the PO of Multiple System Atrophy brains [2, 49]. The significant increase in astrocyte-neuron ratio in AD is likely due to neuronal loss but not to the increase of total number of astrocytes *i.e.* "relative astrocytosis".

To our knowledge this is the first study to estimate the total number of neuroglial cells in the human PO by using unbiased stereological methods. This method is superior to the two-dimensional (2D) approach commonly used in everyday practice, since it is not affected by tissue preparations and shrinkage when the whole structure needs to be analysed. It has been reported repeatedly that changes in cell density assessed by 2D measurements, expressing the number of profiles/per area, do not necessarily reflect changes in total cell numbers [4, 50]. Using stereological methods the data obtained can easily be compared to other similarly designed studies performed in different laboratories, currently using 2D methods. The sum of oligodendrocytes and astrocytes is on the order of 5–10 million per PO while the neuronal number is approximately eight hundred thousand [13].

In conclusion, using a powerful morphometric approach we could be able for the first time to estimate the total number of neuroglial cells in the human PO. These results and those of our previous

study [12] could be used as a morphological groundwork towards the understanding the pathological and pathophysiological processes in AD. The difference in pathological phenotype between PO and "classically" affected brain areas in AD might help to understand the underlying region- and cell-specific pathogenic mechanisms.

Acknowledgement

This work was supported by grants from Stiftelsen Bertil & Gun Stohne, Alzheimer Fond, Karolinska Institute Stiftelse for åldersjukdomar, Stiftelsen för Gamla Tjänarinnor, the Swedish Medical Society and the Swedish Medical Research Council. We thank Janne Näslund for providing us amyloid antibodies and Inga Volkmann for excellent technical support. We want to thank prof Matti Haltia for providing us with a case of presenilin 1 mutation. Furthermore we express gratefulness to all families who donated the brain material for scientific research.

References

1. **Esiri MM, Morris JH.** The neuropathology of dementia. Cambridge University Press. 1997; pp. 80–111.
2. **Jellinger KA.** Cell death mechanisms in neurodegeneration. *J Cell Mol Med.* 2001; 5: 1–17.
3. **Unger JW.** Glial reaction in aging and Alzheimer's Disease. *Microsc Res Tech.* 1998; 43: 24–8.
4. **Giannakopoulos P, Hof PR, Bouras C.** Selective vulnerability of neocortical association areas in Alzheimer's disease. *Microsc Res Tech.* 1998 ;43: 16–23.
5. **Brun A, Liu X, Erikson C.** Synapse loss and gliosis in the molecular layer of the cerebral cortex in Alzheimer's disease and in frontal lobe degeneration. *Neurodegeneration* 1995; 4: 171-7.
6. **Liu X, Erikson C, Brun A.** Cortical synaptic changes and gliosis in normal aging, Alzheimer's disease and frontal lobe degeneration. *Dementia* 1996; 7: 128–34.
7. **Overmyer M, Helisalmi S, Soininen H, Laakso M, Riekkinen P, Alafuzoff I.** Astrogliosis and the ApoE Genotype. *Dem Ger Cogn Dis.* 1999; 10: 252–7.
8. **Whitman GT, Cotman CW**. Oligodendrocyte degeneration in AD. *Neurobiol Aging* 2004. 25: 33–6.
9. **Braak H, Braak E.** Neuropathological stageing of Alzheimer-related changes. *Acta Neuropathol.* 1991; 82: 239–59.
10. **Rub U, Del Tredici K, Schultz C, Thal DR, Braak E, Braak H.** The autonomic higher order processing nuclei of the lower brain stem are among the early targets of the Alzheimer's disease-related cytoskeletal pathology. *Acta Neuropathol. (Berl)*. 2001; 101: 555–64.
11. **Rüb U, Del Tredici K, Schultz C, Thal DR, Braak E, Braak H.** The evolution of Alzheimr's disease-related cytoskeletal pathology in the human raphe nuclei. *Neuropath Appl Neurobiol*. 2000; 26: 553–67.
12. **Braak H and Del Tredici K.** Poor and protracted myelination as a contributory factor to neurodegenerative disorders. *Neurobiol Aging.* 2004; 25: 19–23.
13. **Lasn H, Winblad B, Bogdanovic N.** The number of neurons in the inferior olivary nucleus in Alzheimer's disease and normal aging: A stereological study using the optical fractionator. *JAD.* 2001; 3: 159–68.
14. **Bacci A, Verderio C, Pravettoni E, Mateoli M.** The role of glial cells in synaptic function. *Phil Trans R Soc Lond.* 1999; B354: 403–9.
15. **Dringer R.** Metabolism and functions of glutathione in brain. *Prog Neurobiol.* 2000; 62: 649–71.
16. **Graeber MB, Blakemore WF, Kreutzberg WG.** Cellular pathology of the central nervous system. Greenfield Neuropathology, 7th. Eds Graham DI and Lantos P 2002; pp. 123–92.
17. **Kirchhoff F, Dringer R, Giaume C.** Pathways of neuron-astrocyte interactions and their possible role in neuroprotection. *Eur Arch Psych Clin Neurosci.* 2001; 251: 159–69.
18. **Martinez G, Carnazza ML, Di Giacomo C, Sorrenti V, Avitabile M, Vanella A.** GFAP, S-100β and vimentin proteins in rat after cerebral post-ischemic reperfusion. *Int J Neurosci* 1998; 16: 519–26.
19. **Ventura R and K.M. Harris.** Three-dimensional relationships between hippocampal synapses and astrocytes. *J Neurosci.* 1999; 19: 6897–906.
20. **Pakkenberg B, Pelvig D, Marner L, Bundgaard MJ, Gundersen HJG, Nyengaard JR. Regeur L.** Aging and the human neocortex. *Exp Gerontol*. 2003; 38: 95–9.
21. **Pelvig DP, Pakkenberg H, Regeur L, Oster S, Pakkenberg B.** Neocortical glial cell numbers in Alzheimer's disease. *Dem Ger Cogn Dis.* 2003; 16: 212–9.
22. American psychiatric Association: Committee on Nomenclature and Statistics. Diagnostical and statistical manual of mental disorders 4th edn. Washington DC 1994; 133–45.
23. **McKhann G, Drachmann D, Folstein M, Katzmann R, Price D, Stadlan EM.** Clinical diagnosis of Alzheimer's disease: report of the NINCDS-ADRDA Work group under the auspices of the Department of Health and Human Services; *Neurology* 1984; 34: 939–44.
24. **Bogdanovic N, Morris JH.** Diagnostic criteria for Alzheimer's disease in multicentre brain banking, in: Neuropathological diagnostic criteria for brain banking, Cruz-Sanches FF, Ravid R, Cuzner ML, eds, IOS press, Amsterdam. 1995; 20–9.
25. **Mirra SS, Hart MN, Terry RD.** Making the diagnosis of Alzheimer's disease. *Arch Pathol Lab Med.* 1993; 117: 132–44.
26. **National Institute on Aging and Reagan Institute Working Group on diagnostic criteriafor the neuropathological assessment of Alzheimer disease.;** Consensus recommendations for the post-mortem diagno-

sis of Alzheimer's disease. *Neurobiol Aging.* 1997**;** 18: S1–2.
27. **Näslund J, Haroutunian V, Mohs R, Davis KL, Davies P, Greengard P, Buxbaum JD.** Correlation between elevated levels of amyloid â-peptide in the brain and cognitive decline. *JAMA.* 2000; 283: 1571–7.
28. **Berry M, Butt AM, Wilkin G, Perry VH.** Structure and function of glia in the central nervous system. Greenfield's Neuropathology 7th Ed; 2002.
29. **Dawson TP, Neal JW, Llewellyn L, Thomas C.** Neuropathology techniques. Oxford University press. 2003; pp. 162–79.
30. **West MJ, Slomianka L, Gundersen HJ.** Unbiased stereological estimation of the total number of neurons in the subdivisions of the rat hippocampus using the optical fractionator. *The Anat Rec.* 1991; 231: 482–97.
31**. Gundersen HJG, Jensen EBV, Kieu, K, Nielsen J.** The efficiency of systematic sampling in stereology – reconsidered. *J Microsc*. 1999; 193: 199–211.
32. **Gundersen HJ.** Stereology of arbritrary particles. A review of unbiased number and size estimators and a presentation of some new ones, in memory of William Thompson. *J Microsc.* 1986; 143: 3–45.
33. **Braak H, Braak E**. Demonstration of amyloid deposits and neurofibrillary changes in whole brain sections. *Brain Path.* 1991; 1: 213–6.
34. **Petrova PS, Raibekas A, Pevsner J, Vigo N, Anafi M, Moore MK, Peaire A, Shridhar V, Smith DI, Kelly J, Durocher Y, Commissiong JW.** Discovering novel phenotype-selective neurotrophic factors to treat neurodegenerative diseases. *Prog Brain Res*. 2004; 146: 168–83.
35. **Barres BA, Barde Y-A.** Neuronal and glial cell biology. *Curr Opin Neurobiol.* 2000; 10: 642–8.
36. **Ludwin SK.** The pathology of the oligodendrocyte. *J Neuropathol Exp Neurol.* 1997; 56: 111–24.
37. **Peinado MA.** Histology and histochemistry of the aging cerebral cortex: An overview. *Microsc Res Tech.* 1998; 43: 1–7.
38. **Du Y, Dreyfus CF.** Oligodendrocytes as providers of growth factors. *J Neurosci Res.* 2003; 68: 647–54.
39. **Lee JT, Xu J, Lee JM, Ku G, Han X, Yang DI, Chen S, Hsu CY.** Amyloid-â peptide induces oligodendrocyte death by activating the neutral sphingomyelinase-ceramide pathway. *J Cell Biol.* 2004. 164: 123–31.
40. **Braak H, Braak E.** Development of Alzheimer-related neurofibrillary changes in the neocortex inversely recapitulates cortical myelogenesis. *Acta Neuropathol.* 1996; 92: 197–201.
41. **Iseki E, Matsushita M, Kosaka K, Kondo H, Ishii T, Amano N.** Distribution and morphology of brain stem plaques in Alzheimer's disease. *Acta Neuropath.* 1989; 78: 131–6.
42. **Matsusaka H, Ikeda K, Akiyama H, Arai T, Inoue M, Yagishita S.** Astrocytic pathology in progressive supranuclear palsy: significance for neuropathological diagnosis. *Acta Neuropathol.* 1998; 96: 248–52.
43. **Ikeda K, Akiyama H, Arai T, Kondo H, Haga C, Iritani S, Tsuchiya K.** Alz-50/Gallyas –positive lysosome-like intraneuronal granules in Alzheimer's disease and control brains. *Neurosci Lett*. 1998; 258: 113–6.
44. **Nixon RA, Cataldo AM, Paskevich CA, Hamilton DJ, Wheelock DR, Kanaley-Andrews L.** The lysosomal system in neurons. Involvement at multiple stages of Alzheimer's disease pathogenesis. *Ann NY Acad Sci.* 1992; 674: 65–88.
45. **Nixon RA, Cataldo AM, Mathews PM.** The endosomal-Lysosomal system of neurons in Alzheimer's disease pathogenesis: A review. *Neurochem Res.* 2000; 25: 1161–72.
46. **Nixon RA, Mathews PM, Cataldo AM.** The neuronal endosomal-lysosomal system in Alzheimer's disease. *JAD.* 2 001. 3: 97–107.
47. **Cataldo AM, Barnett JL, Mann DM, Nixon RA.** Colocalization of lysosomal hydrolase and β-amyloid in duffuse plaques of the cerebellum and striatum in Alzheimer's disease and Down's syndrome. *J Neuropathol Exp Neurol*. 1996; 55: 704–15
48. **Cataldo AM, Rebeck GW, Ghetri B, Hulette C, Lippa C, Van Broeckhoven C, Van Duijn C, Cras P, Bogdanovic N, Bird T, Peterhoff C, Nixon R.** Endocytic disturbances distinguish among subtypes of Alzheimer's disease and related disorders. *Ann Neurol.* 2001; 50: 661–5.
49. **Probst-Cousin S, Rickert CH, Schmid KW, Gullotta F.** Cell death mechanisms in multiple system atrophy. *J Neuropathol Exp Neurol.* 1998; 57: 814–21.
50. **Rössler M, Zarski R, Bohl J, Ohm TG.** Stage-dependent and sector-specific neuronal loss in hippocampus during Alzheimer's disease. *Acta Neuropathol.* 2002; 103: 363–9.